

Received February 27, 2020, accepted March 19, 2020, date of publication March 23, 2020, date of current version April 8, 2020.

Digital Object Identifier 10.1109/ACCESS.2020.2982841

A General Framework for Designing 3D Impellers Using Topology Optimization and Additive Manufacturing

E. MELI^{ID}, R. FURFERI^{ID}, A. RIND, A. RIDOLFI^{ID},
Y. VOLPE, AND F. BUONAMICI^{ID}

Department of Industrial Engineering, University of Florence, 50139 Firenze, Italy

Corresponding author: Francesco Buonamici (francesco.buonamici@unifi.it)

This work was supported by the Baker Hughes, a General Electric company (BHGE) Nuovo Pignone.

ABSTRACT Computer Numerical Control (CNC) milling is still today the elective process for the production of single-piece impellers, as it can reliably produce complex geometries, removing the need for additional manufacturing processes. Nevertheless, Additive Manufacturing is winning more and more ground due to its ability to make components of any geometry that cannot be produced using subtractive techniques. As a result, the use of this technology can eventually be seen as the key to develop high-performance rotor components. In this scenario, the design of 3D impellers does not make an exception. Accordingly, the present paper proposes a general framework for engineered re-design and manufacture of 3D impellers installed on centrifugal compressors by exploiting Topology Optimization and Additive Manufacturing's potential. The procedure investigates also the rotoric component's best configuration for both static and dynamic behavior. Finally, the topology-optimized component is produced with AM through the use of suitable materials that can ensure efficient mechanical efficiency to prove the manufacturability of the entire procedure. To validate the proposed framework, the complete re-design of a 3D impeller of a major Italian-based Oil & Gas company is carried out, demonstrating that the re-thinking of the component in terms of Topology Optimization is a straightforward approach to increase the overall performance of the produced rotoric part.

INDEX TERMS 3D impellers, additive manufacturing, design, topology optimization, turbomachinery.

I. INTRODUCTION

To meet the rising demand for energy, designing highly efficient turbomachinery systems [1] is an imperative activity. As a result, Oil & Gas companies are now facing major technological changes to improve their mechanical component quality and overall profitability. Advanced production methods play an important role in reducing costs and developing a fast and efficient approach in this context. This is particularly true when the main aim is to design rotoric turbomachinery components such as, for instance, impellers. The current trend for this type of product is to design products with a reduced number of joined components (ideally single-pieced), thereby avoiding the need for welding processes that require dedicated heat treatments and induce defects and structural distortions in the manufactured product.

The associate editor coordinating the review of this manuscript and approving it for publication was Chi-Tsun Cheng^{ID}.

Computer Numerical Control (CNC) milling is the elective method for single-piece impeller manufacturing, as it can efficiently generate complex geometries using a single production cycle. Nonetheless, there is still a range of drawbacks that the adoption of CNC milling for impeller production entails. Manufacturing times are typically high and increase with the complexity of the surface to produce; moreover, the process requires significant resources: the energy demand is significant and a large-scale waste of good material is produced from the raw component. Furthermore, due to the complexity of the shapes to be created (i.e. hollow objects with several undercuts), the traditional manufacturing process is not straightforward and needs to be carefully planned by technicians.

Some of the above-mentioned issues can be overcome by using the Electrical Discharge Machining (EDM), which is today the elective method used when dealing with impellers characterized by narrow passage and clear flow passage.

This process is well adapted for the manufacture of impellers with very low flow coefficient and ensures high surface performances. Unfortunately, EDM also raises challenges for complex shapes manufacturing and is time-consuming. It should also be noted that the evolution of high-efficiency rotors has led to lighter structures that need to maintain higher speeds. Modern subtractive techniques are less suitable for manufacturing these slender structures, since higher volumes of materials need to be extracted.

Therefore, dealing with rotor parts, the main industrial challenge is to switch from traditional subtractive manufacturing to innovative Additive Manufacturing (AM) processes [2].

Over the last five years, the family of metal AM processes has seen significant improvements in the mechanical quality of the manufactured components, reliability and system predictability. As a result, metal AM processes are now a proven alternative to traditional subtractive processes even for manufacturing mechanical parts that require substantial structural loads to be sustained. However, as documented in [3], AM is still in its early stages for oil and gas applications. Therefore, there is limited scientific literature on the full design and manufacture of turbomachinery components using AM, while a substantial number of works focus only on the manufacturing aspects [4]. Metallurgical aspects of several components, such as super-alloys, were indeed investigated in order to understand AM's potential in the turbomachinery sector [5]. Many literature research deals with smart solutions for a broad variety of applications, including wear of diesel engine exhaust valves [6], corrosion of gas turbine blades [7], mold steel repair [8], wear of high-speed metal tools [9], and many others where conventional methods fail.

All literature work essentially shares the idea that AM allows the creation of single-piece objects whose geometry can be derived from modern design software packages that enable shape optimization. In other words, starting from traditional mathematical surfaces, it is possible to design unconstrained complex geometries and topologies with optimized performances. Topology Optimization (TO) software systems are among the most used design tools in this context. In this type of software, the material distribution within a given design volume can be optimized for a set of loads and boundary conditions thanks to an optimization algorithm so that the resulting layout maximizes an objective function [4]. As a result, TO empowers the designer with great freedom, creating complex structures that cannot be instantly imagined using traditional design methodologies [10].

In [11] the researchers examined TO's potential for designing a 2D impeller mounted on a centrifugal compressor. The results obtained in [11] showed the efficacy of TO and AM approaches for designing innovative rotor components. The encouraging results obtained in such a prior work, prompted to investigate the possibility of applying an integrated method involving TO and AM for the design of 3D impellers i.e. impellers characterized by three-dimensional blades in the radial part [12]. Such a preliminary work

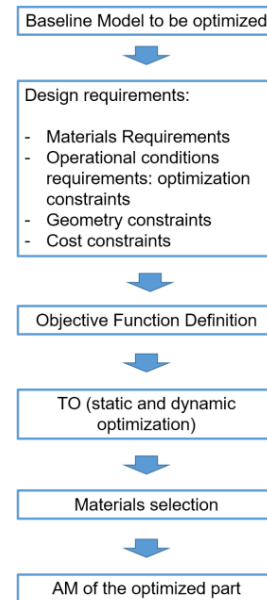


FIGURE 1. Design framework.

successfully applied some TO-based routines to design an effective 2D component, laying the foundation for a more systematic approach. However, in [11], no frameworks are provided to the designers to guide them towards the creation of optimized rotoric parts. Accordingly, the present article extends the previous study by proposing a systematic design procedure which, leveraging the potential of TO and AM, allows the optimal design of any rotoric component used in centrifugal compressors. Moreover, the devised method is particularly suited for designing a new range of 3D impellers.

In the proposed framework, TO is used as a design tool to model 3D impellers, taking into consideration both static and dynamic behavior as well as weight reduction. Once the design of the rotoric component is available, some considerations on its actual manufacturability using AM are drafted. To demonstrate the effectiveness of the proposed workflow, the complete re-design of a 3D impeller of a major Italian-based Oil & Gas company is carried out.

II. DESIGN FRAMEWORK

The design framework, which lead to the design of optimized 3D impellers, is depicted in Figure 1. The starting point of an optimized design of a 3D impeller is a non-optimized disk used as baseline for the subsequent TO.

It consists of a 3D CAD model deriving either from a previous design or from a 3D scanning of existing components. The baseline is used to state a number of functional requirements to be satisfied to assure its correct behavior under operating conditions. Such requirements, stated based on engineers expertise, are translated into a set of optimization constraints. Then, an objective function is defined, whose minimization is the main aim of a constrained optimization routine. After objective function is defined, the TO can take place using an automatic procedure which does not require the human interaction. By implementing one of

the well-established algorithms [13] guiding the optimization process, it is possible to automatically generate a model whose geometry is consistently changed with respect to the baseline model; performance is increased in terms of both static and dynamic behavior. Finally, the optimized model can be manufactured using a metal additive process. To this aim, materials with optimal mechanical characteristics as well as the optimal AM device have to be selected by AM experts. Furthermore, optimal setting of appropriate 3D printing devices are drafted and, on the basis of such parameters, the component is manufactured. The entire framework is detailed in the following sections.

A. BASELINE MODEL

The proposed procedure requires a digital 3D model of the part to be optimized as starting point. Such a 3D model could be either obtained directly from the original design (e.g. it can consist of a CAD drawn model) or by 3D scanning the part and, subsequently, performing a reverse engineering process [14], [15], especially in case the main aim is to re-design existing parts. It is important to highlight that the baseline model is not required to be parametric to accomplish the TO.

B. DESIGN REQUIREMENTS

The rotoric part’s re-design should result in an impeller characterized by high performance. The engineered impeller should therefore adhere strictly to the following requirements. Such requirements are mainly based on the experience of O&G Engineers, who are aware of the stringent mechanical performance required for this kind of product.

1) MATERIALS REQUIREMENTS

Compressors are the engine components responsible for providing adequate air to the combustion chamber with sufficient pressure. Gas turbine engines have two compressors in most cases: low-pressure and high-pressure, running at different operating temperatures. Generally, the low-pressure compressor operates at relatively low temperatures, around 360 ° C, whereas the high-pressure compressor works at temperatures between 480 °C and 600 °C. This means that the 3D impeller should be built with a highly ductile material that can work from up to 600°C.

In addition, it should be resistant to corrosion in the presence of water and CO2 and H2S. It should also have chloride-induced pitting resistance. High performance Inconel alloys meet all these standards when manufactured using subtractive technologies. In particular, the IN718 [16], a precipitation hardenable nickel-based alloy, is characterized by exceptionally high yield, tensile and creep-rupture properties at temperatures up to 700°C, as depicted in Table 1 [11].

The design of the impeller must therefore take into account the use of this type of materials and assure its manufacturability with AM. Moreover, it would be optimal to obtain, using the AM process, a micrographic structure very close to the one obtained by forging the alloy (see Figure 2). For designers

TABLE 1. Mechanical properties of IN718 alloy.

Test Temperature	0.2% Yield Strength	Ultimate Tensile Strength
°C	MPa	MPa
93	1172	1407
204	1124	1365
316	1096	1344
427	1076	1317
538	1069	1276
649	1027	1158
760	758	758

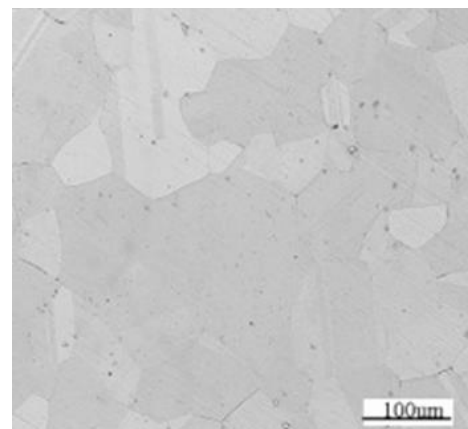


FIGURE 2. Forged IN718 micrographic examination.

aiming to use this kind of material, it is suggested to perform also more extensive metallographic analyses to control the grain size or other mechanical properties of the AM produced parts.

2) OPERATIONAL CONDITIONS REQUIREMENTS

The second set of specifications relates to the operating conditions of a given 3D impeller, which essentially translate into the ability to maintain and endure high-speed stresses. At the same time, weight has to be reduced to limit the centrifugal forces acting on the disk.

Therefore, the optimized design should take into account static and dynamic behavior of the impeller and should aim at reducing weight. This means that the overall static and dynamic performance of the newly designed component should overcome the one obtained for traditional geometries. To confront with this issue, a number of constraints have to be respected during the subsequent optimization routine. The constraints used to guide the optimization are on the displacements, on the maximum value of the stress, on the volume fraction and on modes frequency. In detail, the following requirements have to be met:

$$\begin{cases} \sigma_{max} < \sigma_r \\ u_{max} < u_r \\ V_{fr,min} < V_{fr} \\ freq_{m_i} < freq_{\hat{m}_i} - \Delta_{freq} \\ freq_{m_j} > freq_{\hat{m}_j} + \Delta_{freq} \end{cases} \quad (1)$$

where:

σ_{max} is the maximum values of stress in the optimized model, assessed using a Finite Element Analysis.

σ_r is the maximum allowable value of stress for the optimized model. This value has to be set by the designer.

u_{max} is the maximum interference area radial displacements.

u_r is the maximum radial displacements to be set during the optimization test; u_r should be lower than the corresponding one in the baseline model.

$V_{fr,min}$ is the minimum volume fraction for the optimized model, that is introduced to avoid the whole part deletion by the solver (see optimization procedure).

V_{fr} is the minimum design volume fraction to be set in the topology optimization test. This value can be set by the designer. Typically, it varies in the range 10% - 20%, measured on the outer disk of the rotoric component. The volume fraction is defined as the ratio of the difference between the current iteration total volume and the initial volume of non-design to the initial volume of design. This constraint is enforced to ensure that a volume fraction remains permanent in a particular part: in short, this restriction is placed on the outer disk to prevent the solver from completely removing this part.

$freq_{m_i}$ is the frequency response of the i^{th} mode of the optimized model which is lower to the operating range.

$freq_{\hat{m}_i}$ is the frequency response of the i^{th} mode of the baseline model which is lower to the operating range.

$freq_{\hat{m}_j}$ is the frequency response of the j^{th} mode of the baseline model which is greater to the operating range.

$freq_{m_j}$ is the frequency response of the j^{th} mode of the optimized model which is greater to the operating range.

Δ_{freq} is a threshold frequency value to be subtracted or added to the baseline modes frequency to define the optimized modes frequency. If, for instance, $\Delta_{freq} = 200 \text{ Hz}$, this means that the frequencies of all the modes around the operational conditions are required to be shifted 200 Hz above or below the current value so that the frequencies of the vibrational modes around it are kept apart.

3) GEOMETRY CONSTRAINTS

As mentioned above, the main aim is to devise a framework able to perform an optimization of the topology of any kind of 3D impeller. This means that certain specific areas, i.e. the original impeller's shape must be significantly changed in order to reduce weight, improve strength efficiency and minimize displacements. However, the redesign process should take into account that there are geometry constraints to be respected. Certain 3D impeller regions are required to remain unchanged in the final configuration of any newly defined optimized geometry. Typically, the blade region is the one which must be preserved since its geometry derives from fluid dynamic optimizations (whose study is not covered by this paper). Therefore, such an area belongs to the non-design space. The rest of the impeller can be viewed as part of the design space and can therefore be subject to dramatic

changes during the optimization routine. It is a designer effort to define the proper design space, depending on their own definition of the area to be optimized.

4) COST REQUIREMENTS

The final requirement is referred to reduction of production costs. The design of the impeller should consider the possibility of reducing as much as possible the cost of the manufacturing, albeit in the knowledge that AM is more expensive than the traditional subtractive process. This means that commercially available 3D printers have to be selected for the production of the component. In this case, the cost of low-volume production runs has been shown to be lower than traditional production techniques, especially when less than 100 units are produced. Lead times are also more favorable for such components, being on the scale of weeks instead of months. Accordingly, the increase of performance, when combined with the need to manufacture a limited number of parts may lead to an advantageous use of AM in turbomachinery. When production volume exceeds one hundred units, a cost-benefit analysis should be performed to verify the sustainability of the production choices in terms of performance improvements vs. costs.

C. OBJECTIVE FUNCTION DEFINITION

To carry out an effective TO, it is necessary to define, in a first instance, a proper Objective Function to be minimized, without violating in any case the above-mentioned constraints. For rotoric components, the typical Objective Functions adopted in literature are: *overall volume* $V(\rho_f)$ and *compliance* $L(\underline{u})$. The *overall volume* has a simple formulation, as shown in Equation 2:

$$V(\rho_f) = \int_{\Omega} \rho_f d\Omega \quad (2)$$

where ρ_f is the (dimensionless) material density and Ω is the optimization domain i.e. the design space defined in Section 1.2.3. Unfortunately, it has been demonstrated that the minimization of such function may lead to convergence problems, which produce irregular final geometries. Consequently, the best choice for optimizing 3D impellers, may be considered the *compliance*. It is defined as the strain energy of the part i.e. the reciprocal measure of the stiffness of the structure, as described by the following equation:

$$L(\underline{u}) = \int_{\Omega} \underline{f} \cdot \underline{u} d\Omega + \int_{\Gamma_T} \underline{t} \cdot \underline{u} ds \quad (3)$$

where: \underline{f} are the body forces (centrifugal load in this work) on the domain Ω ; \underline{t} are the boundary tractions on the traction part $\Gamma_T \subset \partial\Omega$ and \underline{u} are the displacements in the area of interference between the shaft and impeller. Minimizing compliance means finding the material density distribution under the chosen boundary and loading conditions that minimizes structural deformation. As stated in Section 1.3, the only considered load for this kind of impellers is the centrifugal

force field. Therefore, body forces are defined by:

$$\underline{f} = \rho \omega^2 \begin{pmatrix} x \\ y \\ 0 \end{pmatrix} \quad (4)$$

where ρ is the material density and ω is the rotational speed of the 3D impeller. It has to be noticed that the rotation axis of the disk is referred to z axis; therefore, the centrifugal force depends only on x and y coordinates of the disk.

Finally, the OF is given by:

$$L(\underline{u}) = \int_{\Omega} \rho \omega^2 \begin{pmatrix} x \\ y \\ 0 \end{pmatrix} \cdot \underline{u} \, d\Omega + \int_{\Gamma_T} \underline{t} \cdot \underline{u} \, ds \quad (5)$$

D. TOPOLOGY OPTIMIZATION

A number of strategies and algorithms can be applied to minimize $L(\underline{u})$, including Discrete method, method with continuous variables, Phase field and Solid Isotropic Material with Penalization (SIMP) [13]. The preferred method for the re-design of 3D impellers is the SIMP approach [17]. Through this density-based method, a pseudo material density ρ_f can be used as the design variable. During the optimization procedure, ρ_f of each element varies continuously between 0 and 1; the *void* condition is identified by a zero-density value as no material is present in that point while points marked as “1” are characterized by solid material. Intermediate values represent the density of a “fictitious material” whose mechanical properties are influenced by the density itself. For the relationship between stiffness and density, the SIMP method applies a power-law penalization to set density to 0 and 1 distribution. The material’s stiffness is supposed to be linearly density-dependent. In general, large areas with intermediate densities in the structural domain are involved in the optimal solution of problems. As a consequence, a penalization technique has to be performed to push the final design to represent 0 or 1 densities for each element. The most useful penalization technique is the so-called “power law representation” of elasticity properties, provided by Equation 6:

$$E = E_0 [\rho^p] \quad (6)$$

where:

E is the optimum young modulus of the topology element;

E_0 represents the young modulus of the initial design space material;

p is the penalty factor applied to the density to control the generation of intermediate density elements (high, medium and low porosity);

It should be noted that using the SIMP formulation to solve the OF of Equation 5, the dynamic loads are considered in the optimization procedure only in terms of frequency constraints, to keep the modal frequencies of the optimized system away from the machine’s most common frequency operating range. At the same time, since the operating conditions of the system at such frequency during the machine

life may be quite complex and different from the nominal, it is not suggested to apply a dynamic load on the compressor blades in terms of the harmonic pressure field. In fact, this harmonic stress field would be connected to a particular working condition of the machine and not fully representative of the pressure loads operating on the machine throughout its lifetime. The entire TO process can be carried out without user interaction.

Moreover, a complete thermo-structural optimization (involving the optimization of temperature and thermal flux, computationally much heavier) is not reported in this work. Nonetheless, complex statistical and experimental fluid dynamic analyses can be performed “a posteriori” to check the performance of engineered components under different operating conditions.

E. MATERIALS SELECTION

As already stated, it is not possible to assure the manufacturability of the generated geometry using conventional subtractive technology. Therefore, AM must be implemented to produce 3D optimized impellers under any circumstance. In particular, metal AM is the obvious choice to assure satisfying mechanical performance of the component. Two main technologies are capable of producing 3D printed parts while assuring performances comparable to forged materials: Direct Metal Laser Sintering (DMLS) and Electron Beam Melting (EBM). The former is an additive manufacturing technique able to fuse together fine powder layers using a laser beam. Since parts are manufactured with 95% density the DLMS process does not require any subsequent sintering of the produced parts. Parts may require a variety of post processes, including heat-treating, support removal, shot peening, and more. In EBM, a similar process, implementing the raw material (metal powder or wire) is placed under a vacuum and fused together from heating by an electron beam.

Both technologies are able to process the same material adopted for standard rotoric parts like, as already mentioned, the IN718. However, the microstructure obtained for both processes may differ significantly from the alloy’s forged version; there is also no guarantee that the mechanical and chemical properties will be the same. Therefore, a characterization of the 3D printed material both in terms of physical resistance (strength, ultimate tensile strength UTS, % elongation to rupture) and of corrosion resistance (CO₂, water and H₂S corrosion resistance) are required. Authors suggest to carry out such a characterization using dedicated test according NACE recommendations [18]. In the present work, a characterization of parts specimens created using the DMLS process was carried out. In detail, a thorough investigation focused on the printed material’s fatigue and tensile properties, specifically compared to the equivalent forged alloy.

Comparison revealed that the DMLS sample has a better ductile nature with respect to the forged one, i.e. at lower temperature it has higher elongation and lower UTS. In any case, the sintered parts still respect the requirements in terms of material properties stated in Section 1.2.1 as demonstrated

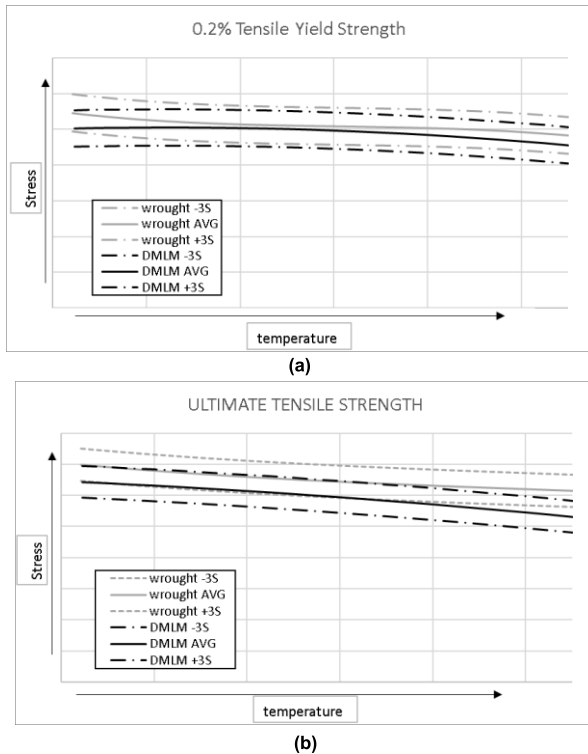


FIGURE 3. a) 0.2% Tensile yield strength comparison between sintered specimen and forged one; b) UTS comparison between sintered specimen and forged one.

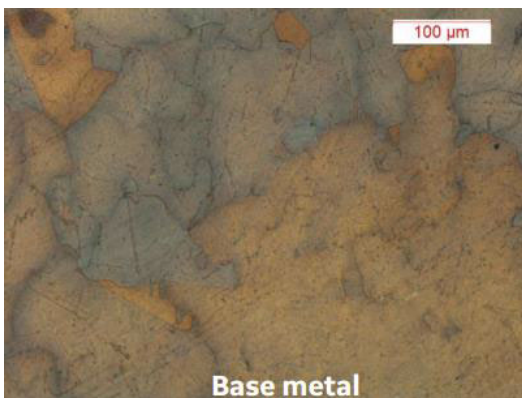


FIGURE 4. DMLS IN718 micrographic examination.

in Figure 3. Variability in the DMLS process can be compared to the forging process since the statistically processed data shows approximately the same standard deviation for both processes. Furthermore, a metallographic examination of DMLS samples demonstrate a visually similar material grain size and disposition of the base material when compared with forged one (see Figure 4).

In summary, it is possible to prove that the 3D printed IN718 can be considered as a very good alternative to forgings, at least for part sizes within printable dimensions, as scientific literature has also shown [16]. Additional tests showed that high-precision DMLS parts have good surface characteristics along with mechanical properties equal to those seen in

traditional materials, particularly after proper heat treatment has been performed [19].

F. ADDITIVE MANUFACTURING

After the metal characterization has been done and the mechanical properties of the material confirmed, the engineered part can be produced. As already mentioned, the selected technology is the DMLS. Since it is possible to move the print bed in increments of as little as 20 microns, objects have a smooth surface quality that minimizes the need for finishing post-production.

The guidelines to correctly manufacture a prototype using DMLS are the followings:

- Definition of the model position and orientation within the machine build volume. To reduce the incidence of thermal deformations and residual stresses on the fabricated component, this step should be carried out carefully. In fact, the direction of the component can also influence surface quality: this factor should be taken into account in order to reduce the need for post-processing operations.
- Metal powder deposition and melting for the DMLS process, tuned to enhance the geometric performance of the part.
- Heat treatment of the part produced by the AM process to reduce deformation.
- Elimination of the internal support necessary to maintain an angle above 45° overhanging structures.
- Final machining of the external geometry.
- Finishing process to reduce the flow path region's final roughness.

It is up to expert AM users to follow the above-mentioned guidelines to carry out the optimal manufacturing of the optimized part.

III. CASE STUDY

The proposed framework was tested to design a 3D impeller currently mounted on a centrifugal processor by GE Company. The framework of Figure 1 is declined for the considered case study in the flow of Figure 5.

A. BASELINE MODEL

The baseline model is the digital counterpart of the 3D impeller of Figure 6, the main specifications of which are in Table 2.

The baseline part (Figure 7) has linear elastic isotropic properties, as listed in Table 3.

B. DESIGN REQUIREMENTS

The design of the new impeller has to satisfy the requirements in terms of materials and cost stated in the general procedure. For what concerns the operational conditions, the standard component performance was verified by means of a Finite Element Analysis (FEA) to estimate both the maximum displacement and the maximum stress of the impeller.

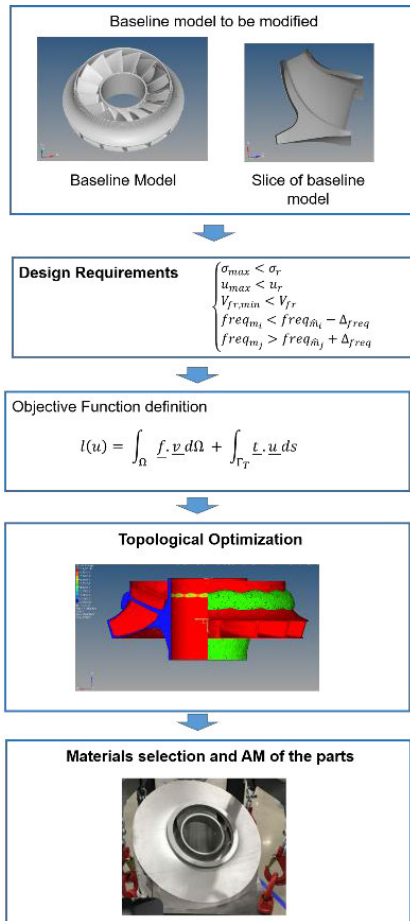


FIGURE 5. Design Framework for the case study.

The FE-based simulation was performed using the only static loading condition due to a centrifugal force field, as external load applied to the rotating part. The rotational velocity ω is set to 15120 rpm (252 Hz) which is the speed at full capacity for this specific rotor. The whole part's symmetry (15 identical vanes) allowed a simpler analysis to be carried out only on a part's circular 24° field where cyclic symmetry constraints are applied. The results of the FEA are in Figure 8 and in Table 4.

Alongside to some hot spots that are created by stress concentration factors caused by the rotoric component's particular geometry, a general stress gradient that moves from the internal to the external radius can be identified. Such stress condition is fully compatible with the considered application.

The impeller was also characterized by a modal analysis. In fact, the main objective for the subsequent TO is to transfer different vibrating modes away from the operating range. This means that frequencies have to be moved away from the frequency range near the working frequency ω_w :

$$\omega_w = N * \omega = 3780Hz \tag{7}$$

where $N = 15$ is the number of vanes.

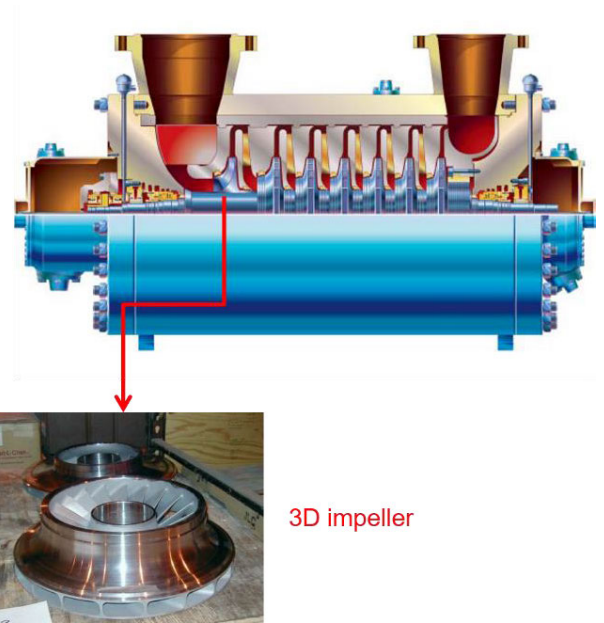


FIGURE 6. 3D impeller from a centrifugal compressor.

TABLE 2. Specifications of the case-study impeller.

Flow Coefficient	0.16
Mach	1.00
External Diameter [mm]	390
Vane number	15

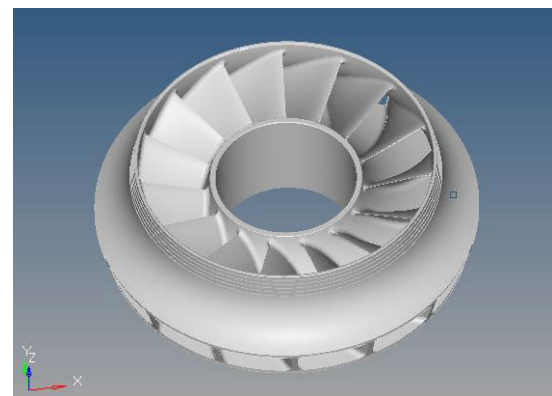


FIGURE 7. Baseline model.

TABLE 3. Material properties.

Young's Modulus (E)	$2.2 \cdot 10^5$ MPa
Poisson's Ratio (ν)	0.3
Density (ρ)	$7.85 \cdot 10^3$ kg/m ³

Table 5 shows the natural modes of the test case impeller 4. The modes from 9 to 13 are dangerously close to the operating range and should be kept outside the range itself with a minimum margin Δ_{freq} . In this case study, Δ_{freq} is set to the value 300 Hz.

From the above FEA, it is possible to derive, finally, the constraints of the Optimization Problem; the selected value

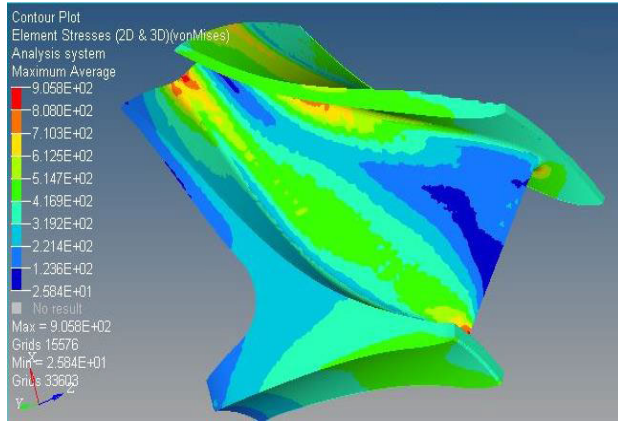


FIGURE 8. Von Mises ultimate tensile strength on a vane of the 3D impeller.

TABLE 4. Maximum stress and maximum radial displacement for the baseline model.

Ultimate tensile strength [MPa]	905
Maximum displacement [mm]	0.17
(data refers to the interference region between impeller and shaft)	

TABLE 5. 3D disk natural modes.

Mode	Baseline model Frequency [Hz]	Notes
1	1544	
2	1717	
3	1718	
4	2085	
5	2086	
6	2365	
7	2366	
8	2540	
9	3376	Frequencies close to the operational range ω_w , equal to 3780 Hz
10	3377	
11	3397	
12	3398	
13	3400	
14	4735	
15	4736	
16	4963	

for V_{fr} is set to 20%.

$$\begin{cases} \sigma_{max} < 905MPa \\ u_{max} < 0.17mm \\ V_{fr,min} < 20\% \\ freq_{m_i} < freq_{\hat{m}_i} - 300Hz \\ freq_{m_j} > freq_{\hat{m}_j} + 300Hz \end{cases} \quad (8)$$

As mentioned above, the introduction of modal constraints is useful to move away some vibrating modes from the operating range (e.g. modes from 9 to 13 listed in Table 5 should be kept outside the operating range with a margin of at least 300 Hz).

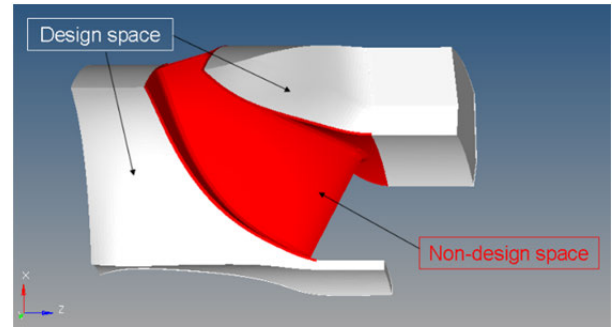
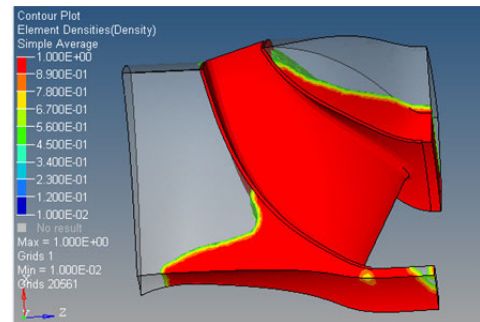
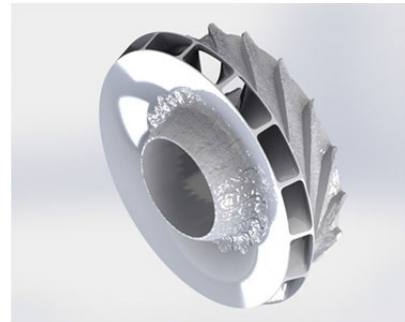


FIGURE 9. Geometry constraints for a 3D impeller.



(a)



(b)

FIGURE 10. (a) static and modal TO; b) CAD model of the optimized 3D impeller.

Referring to geometry constraints, as already stated the blade region must be preserved. Figure 9 illustrates the disposition of design and non-design space (white volumes represent the design space, while the red ones are the non-design space).

C. OBJECTIVE FUNCTION DEFINITION

The selected Objective Function (OF) to be minimized during optimization is the *compliance* as defined by Equation 5.

D. STATIC AND MODAL TOPOLOGY OPTIMIZATION

TO was carried out in Altair HyperWorks environment by using the SIMP method. Figure 10a shows the best performance for static and modal topological optimization. Figure 10b shows the CAD model of the optimized 3D impeller. Red regions are the unit density zones, while no results volumes are no density respectively no material vol-

TABLE 6. 3D impeller optimization results.

	Baseline	Optimization	Reduction
Maximum stress [MPa]	905	680	25%
Maximum displacement [mm]	0.17	0.14	17%

TABLE 7. 3D impeller optimization results.

Mode	Benchmark Frequency [Hz]	Optimized Frequency [Hz]
1	1544	967
2	1717	967
3	1718	1003
4	2085	1449
5	2086	1449
6	2365	1514
7	2366	1514
8	2540	1868
9	3376	2291
10	3377	2291
11	3397	2778
12	3398	2779
13	3400	2900
14	4735	4040
15	4736	4190
16	4963	4199

umes. Table 6 lists values of peak pressure and radial displacement. Both von Mises’ maximum stress and maximum displacement were significantly reduced, thereby confirming the newly designed impeller’s optimized mechanical behavior.

The results in terms of modes are summarized in Table 7. All the constraints in terms of frequency and stress are respected and the overall mass of the impeller is reduced by almost 30%. Frequencies around the operational range are also optimized. In particular, mode 13 frequency is reduced to a value less than 3000 Hz and frequency 14 is higher than 4000 Hz.

It should also be pointed out that the algorithm has removed mass at a higher diameter zone, which is the area that vibrates more, which reduces the structure’s stiffness. At the same time, a series of reinforcements along the blade tip are created to keep the stress level below 900 MPa, along with a concentration of mass on the eye region above the leading edge of the blade

It is important to note that the objective is to perform the structural optimization of the component in this phase of the research activity. The dependence on the temperature of the material characteristics (thermal expansion, Young modulus, etc.) was considered but the working temperature was kept constant.

E. ADDITIVE MANUFACTURING OF THE COMPONENT

The machine used to create the prototypes is the EOS M400, with a 400 × 400 × 400 mm volume capacity. It is important to note that unusual geometries characterize the designed component, also due to the low flow coefficient

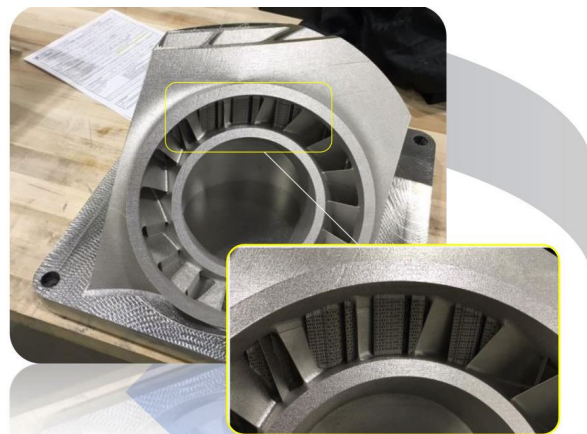


FIGURE 11. Final prototype of the impeller.

(i.e. below 0.2) that includes very narrow blade passages. With this respect, possible improvements on the printability of the produced shape could be achieved by introducing manufacturing constraints within the design procedure, possibly directly in the optimization routine as in [20].

By following the guidelines stated in Section 1.6, it is possible to print in 3D the impeller. Machine parameters were tuned according to the set of guidelines provided in [21]. Moreover, suggestions from literature studies [22], [23] on the effect of the DMLS settings and on the positioning of the part were considered to capitalize on the desired mechanical and geometrical properties. The positioning of the disk should be determined pursuing a tradeoff between the minimization of support structures (which for this type of components is usually obtained with the disk oriented at 45° from the horizontal plane) and the reduction and uniformization of residual stresses within the component (a symmetrical orientation of the disk w.r.t. the machine axes would be beneficial to this aspect). Heat treatment is essential for the reduction of residual stresses (which are, in some measure, always present); HIP and annealing are among the techniques typically applied in such circumstances.

The final re-designed 3D impeller, which is compliant with the set of specifications stated in the premises [24] is depicted in Figure 11.

IV. CONCLUSION

This paper proposed a general framework for engineered re-design and manufacture of 3D impellers installed on centrifugal compressors by exploiting Topology Optimization and Additive Manufacturing’s potential. Starting from the 3D model of an existing impeller and defining a set of functional and geometric requirements, the proposed framework provides a set of guidelines to re-design the part to optimize its performance. The results reported for the case study of a 3D impeller designed by an Italian company operating in the oil & gas sector showed how topological optimization is capable of delivering optimal results in terms of mass reduction, stress optimization of the structure’s dynamic response. Significant changes in mechanical efficiency were achieved:

as compared to traditional model, the strain values and the radial displacements of the interference area are lowered and the impeller weight also decreased.

In respect to future improvements, numerical and experimental fluid dynamical analyses will be carried out to check the structural properties of engineered components under different operating conditions [25]. Moreover, a complete thermo-structural design will be conducted for analog rotoric devices and components operating at higher temperatures. This task could be dealt with effectively by applying multi-objective optimization strategies [26].

Overall, optimizing the entire production process (structural optimization – additive manufacturing – post AM treatments) will be the main goal of the new research steps. To this end, consideration will be given to new and more extreme structural optimization techniques. Interesting direction, with this respect, would be the integration of multiple aspects within a single optimization in order to couple thermo-fluido-structural behavior of the component. The ultimate goal would be the identification of an optimal shape that maximizes many functional requirements at the same time. Furthermore, additional advantages could be achieved by integrating lattice topology in the TO process in order to maximize the structural efficiency of the proposed solution.

ACKNOWLEDGMENT

The authors would like to thank BHGE Nuovo Pignone, a major Italian-based Oil & Gas company, that worked with the authors in identifying a significant case study.

REFERENCES

- [1] X. Lei, M. Qi, H. Sun, and L. Hu, "Investigation on the shock control using grooved surface in a linear turbine nozzle," *J. Turbomach.*, vol. 139, no. 12, Dec. 2017, Art. no. 121008.
- [2] J. M. J. Netto and Z. D. C. Silveira, "Design of an innovative three-dimensional print head based on twin-screw extrusion," *J. Mech. Des.*, vol. 140, no. 12, pp. 1–6, Dec. 2018, Art. no. 125002.
- [3] G. Fayaz and S. Kazemzadeh, "Towards additive manufacturing of compressor impellers: 3D modeling of multilayer laser solid freeform fabrication of nickel alloy 625 powder mixed with nano-CeO₂ on AISI 4140," *Additive Manuf.*, vol. 20, pp. 182–188, Mar. 2018.
- [4] A. W. Gebisa and H. G. Lemu, "Additive manufacturing for the manufacture of gas turbine engine components: Literature review and future perspectives," in *Proc. Ceramics; Controls, Diagnostics, Instrum.; Educ.; Manuf. Mater. Metall.*, vol. 6, 2018, Art. no. V006T24A021.
- [5] C. Boig, M. Burkinshaw, C. Boig, and I. Todd, "The application of additive manufacturing to turbomachinery," in *Proc. 13th Int. Conf. Turbochargers Turbocharging Inst. Mech. Eng.*, 2018, pp. 261–269.
- [6] C. Navas, A. Conde, M. Cadenas, and J. de Damborenea, "Tribological properties of laser clad stellite 6 coatings on steel substrates," *Surf. Eng.*, vol. 22, no. 1, pp. 26–34, Feb. 2006.
- [7] H. Wang, D. Zuo, X. Li, K. Chen, and M. Huang, "Effects of CeO₂ nanoparticles on microstructure and properties of laser clad Ni-CrAlY coatings," *J. Rare Earths*, vol. 28, no. 2, pp. 246–250, Apr. 2010.
- [8] C. Navas, A. Conde, B. J. Fernández, F. Zubiri, and J. de Damborenea, "Laser coatings to improve wear resistance of mould steel," *Surf. Coat. Technol.*, vol. 194, no. 1, pp. 136–142, Apr. 2005.
- [9] W. Darmawan, J. Quesada, F. Rossi, R. Marchal, F. Machi, and H. Usuki, "Improvement in wear characteristics of the AISI M2 by laser cladding and melting," *J. Laser Appl.*, vol. 21, no. 4, pp. 176–182, Nov. 2009.
- [10] M. E. Orme, M. Gschweil, M. Ferrari, I. Madera, and F. Mouriaux, "Designing for additive manufacturing: Lightweighting through topology optimization enables lunar spacecraft," *J. Mech. Des.*, vol. 139, no. 10, Oct. 2017, Art. no. 100905.
- [11] E. Meli, A. Rindi, A. Ridolfi, R. Furferi, F. Buonamici, G. Iurisci, S. Corbò, and F. Cangioli, "Design and production of innovative turbomachinery components via topology optimization and additive manufacturing," *Int. J. Rotating Machinery*, vol. 2019, pp. 1–12, Sep. 2019.
- [12] Y. Galerkin, A. Reksrin, and A. Drozdov, "2D and 3D impellers of centrifugal compressors—advantages, shortcomings and fields of application," *IOP Conf., Mater. Sci. Eng.*, vol. 232, Aug. 2017, Art. no. 012040.
- [13] G. I. N. Rozvany, "A critical review of established methods of structural topology optimization," *Struct. Multidisciplinary Optim.*, vol. 37, no. 3, pp. 217–237, Jan. 2009.
- [14] F. Buonamici, M. Carfagni, and Y. Volpe, "Recent strategies for 3D reconstruction using reverse engineering: A bird's eye view," in *Advances on Mechanics, Design Engineering and Manufacturing (Lecture Notes in Mechanical Engineering)*, 2017, pp. 841–850, doi: 10.1007/978-3-319-45781-9_84.
- [15] F. Buonamici and M. Carfagni, "Reverse engineering of mechanical parts: A brief overview of existing approaches and possible new strategies," in *Proc. ASME Design Eng. Tech. Conf.*, 2016, pp. 1–7, Paper DETC2016-59242, V01BT02A003, doi: 10.1115/DETC2016-59242.
- [16] INCONEL Alloy 718. [Online]. Available: <http://www.specialmetals.com>
- [17] M. P. Bendsoe, "Optimal shape design as a material distribution problem," *Struct. Optim.*, vol. 1, pp. 193–202, Dec. 1989.
- [18] *Corrosion Basics—NACE*. Accessed: Jul. 9, 2019. [Online]. Available: <https://www.nace.org/resources/general-resources/corrosion-basics>
- [19] L. E. Murr, "Metallurgy of additive manufacturing: Examples from electron beam melting," *Additive Manuf.*, vol. 5, pp. 40–53, Jan. 2015.
- [20] Y. Tang, G. Dong, Q. Zhou, and Y. F. Zhao, "Lattice structure design and optimization with additive manufacturing constraints," *IEEE Trans. Autom. Sci. Eng.*, vol. 15, no. 4, pp. 1546–1562, Oct. 2018.
- [21] F. Calignano, D. Manfredi, E. P. Ambrosio, L. Iuliano, and P. Fino, "Influence of process parameters on surface roughness of aluminum parts produced by DMLS," *Int. J. Adv. Manuf. Technol.*, vol. 67, nos. 9–12, pp. 2743–2751, Aug. 2013.
- [22] P. F. Kelley, A. Saigal, J. K. Vlahakis, and A. Carter, "Tensile and fatigue behavior of direct metal laser sintered (DMLS) inconel 718," in *Proc. Volume 2A, Adv. Manuf.*, Nov. 2015, pp. 1–9, Paper IMECE2015-50937, V02AT02A001.
- [23] Q. Shi, D. Gu, M. Xia, S. Cao, and T. Rong, "Effects of laser processing parameters on thermal behavior and melting/solidification mechanism during selective laser melting of TiC/Inconel 718 composites," *Opt. Laser Technol.*, vol. 84, pp. 9–22, Oct. 2016.
- [24] S. Khodaygan and A. Ghaderi, "Tolerance–reliability analysis of mechanical assemblies for quality control based on Bayesian modeling," *Assem. Automat.*, vol. 39, no. 5, pp. 769–782, Nov. 2019, doi: 10.1108/AA-06-2018-081.
- [25] C. Juillet, A. Oudriss, J. Balmain, X. Feaugas, and F. Pedraza, "Characterization and oxidation resistance of additive manufactured and forged IN718 ni-based superalloys," *Corrosion Sci.*, vol. 142, pp. 266–276, Sep. 2018.
- [26] B. Xin, L. Chen, J. Chen, H. Ishibuchi, K. Hirota, and B. Liu, "Interactive multiobjective optimization: A review of the state-of-the-art," *IEEE Access*, vol. 6, pp. 41256–41279, 2018.



E. MELI received the Ph.D. degree in theory of machines and mechanisms from the University of Bologna, Bologna, Italy, in 2010.

He is currently an Assistant Professor in machine theory at the School of Engineering, Florence University, Florence, Italy. His current research interests include rotor dynamics, turbomachinery, structural optimization and additive manufacturing, vehicle dynamics, and tribology.



R. FURFERI is currently an Assistant Professor at the Department of Industrial Engineering, University of Florence, Italy, where he teaches the mechanical drafting course. His main research activities are computer-based methods and tools, 2D and 3D machine vision for industrial process and product control and inspection, geometric modeling, CAD, and computational graphics. In these areas, he has authored more than 70 publications in scientific journals and refereed conference proceedings.



A. RIDOLFI graduated in mechanical engineering from the University of Florence (UNIFI), in 2010, where he also received the Ph.D. degree in industrial engineering, in 2014. At the beginning of his Ph.D., he worked on railway vehicle localization and wheel-rail adhesion modeling. He is currently a Ph.D. Researcher (Assistant Professor) of machine theory and robotics with the Department of Industrial Engineering (DIEF), School of Engineering, University of Florence (UNIFI), Italy. His current research interests are underwater and industrial robotics, sensor-based navigation of vehicles, mechanical systems modeling, vehicle dynamics, and bio-robotics. He worked as a Researcher and an Assistant of the Coordinator within the FP7 European Project ARROWS (ARchaeological ROBot systems for the World's Seas), from 2012 to 2015. He is the Principal Investigator for UNIFI in the framework of two European projects on marine robotics. He has coauthored more than 100 scientific articles for international journals and conferences on robotic and mechatronic topics, with particular focus on underwater robotics. He currently teaches a course in "Dynamics" at Syracuse University, Florence (Spring semester only), where he serves as an Adjunct Professor.



A. RIND was born in Florence, Italy, in March 1967. He graduated in mechanical engineering from the University of Florence, in July 1996. He received the Ph.D. degree (*cum laude*) in applied mechanical from the University of Bologna, in April 2000.

From May 2000 to November 2002, he has been a Temporary Research Assistant with the Department of Energetic "S.Stecco" of the University of Florence and was involved in the research program Brite-EuRam III VERT (Vehicle Road Tyre Interaction), funded by the European Community. He became a Researcher at the University of Florence, in November 2002, where he became an Associate Professor, in March 2018. He currently holds some courses mainly regarding applied mechanics and vehicle modeling at the Faculty of Engineering, Florence University. He also holds two master's courses in the "road safety" and "advanced mechanical design" at Florence University. He develops an intense research activity on themes related to mechanical modeling, especially through multibody techniques, and dynamic simulation of both railway and road vehicles. He has also interests on vehicle control systems topics.



Y. VOLPE is currently an Assistant Professor at the Department of Industrial Engineering, University of Florence, Italy, where he teaches the course CAD modeling at the School of Engineering. He has authored more than 50 journal articles and refereed conference proceedings. His research works are 3D modeling, mechanical design, computational geometry, human-computer interaction, and reverse engineering.



F. BUONAMICI received the M.S. degree in mechanical engineering and the Ph.D. degree in industrial engineering at the University of Florence, in 2014 and 2018, respectively. He is currently a Postdoctoral Research Fellow at the Department of Industrial Engineering of Florence, Italy. His research interests focus on reverse engineering, rapid prototyping, CAD modeling, and industrial design.

...